

Article

# Multi-Level Simulation Framework for Degradation-Aware Operation of a Large-Scale Battery Energy Storage Systems

Leon Tadayon  and Georg Frey \* 

Chair of Automation and Energy Systems, Saarland University, 66123 Saarbrücken, Germany;  
leon.tadayon@aut.uni-saarland.de

\* Correspondence: georg.frey@aut.uni-saarland.de

**Abstract:** The increasing integration of renewable energy sources necessitates efficient energy storage solutions, with large-scale battery energy storage systems (BESS) playing a key role in grid stabilization and time-shifting of energy. This study presents a multi-level simulation framework for optimizing BESS operation across multiple markets while incorporating degradation-aware dispatch strategies. The framework integrates a day-ahead (DA) dispatch level, an intraday (ID) dispatch level, and a high-resolution simulation level to accurately model the impact of operational strategies on state of charge and battery degradation. A case study of BESS operation in the German electricity market is conducted, where frequency containment reserve provision is combined with DA and ID trading. The simulated revenue is validated by a battery revenue index. The study also compares full equivalent cycle (FEC)-based and state-of-health-based degradation models and discusses their application to cost estimation in dispatch optimization. The results emphasize the advantage of using FEC-based degradation costs for dispatch decision-making. Future research will include price forecasting and expanded market participation strategies to further improve and stabilize the profitability of BESS in multi-market environments.

**Keywords:** battery energy storage system; multi-level simulation framework; cross-market participation; degradation-aware operation



Academic Editors: Andrea Trovò and Walter Zamboni

Received: 7 April 2025

Revised: 8 May 2025

Accepted: 14 May 2025

Published: 23 May 2025

**Citation:** Tadayon, L.; Frey, G. Multi-Level Simulation Framework for Degradation-Aware Operation of a Large-Scale Battery Energy Storage Systems. *Energies* **2025**, *18*, 2708. <https://doi.org/10.3390/en18112708>

**Copyright:** © 2025 by the authors. Licensee MDPI, Basel, Switzerland. This article is an open access article distributed under the terms and conditions of the Creative Commons Attribution (CC BY) license (<https://creativecommons.org/licenses/by/4.0/>).

## 1. Introduction

The global transition from fossil fuels to more sustainable energy sources is leading to rapid growth in installed renewable energy capacity, particularly wind and solar. While these technologies offer emission-free energy generation, their output is highly variable, making it difficult to accurately plan the amount of energy that will be produced. Today, flexible power generation is mainly provided by conventional thermal power plants, which produce a significant amount of emissions. The key solution to this problem is to store excess renewable energy when it is abundant and use it at times when wind and solar energy production is low. One of the most promising storage technologies for this application is battery energy storage systems (BESS) [1]. These storage systems can be built on a large scale with an energy capacity exceeding  $\geq 1$  MWh [2] and can interact directly with electricity markets. Lithium-based batteries are the dominant cell type for batteries in this application due to their rapidly decreasing cost [1].

### 1.1. Literature Review

These energy storage solutions have already been widely covered in the academic literature with their various applications, which can be divided into behind the meter

(BTM) and front of the meter (FTM) [3]. The BTM application primarily creates value on the consumer side through peak shaving or self-consumption optimization, while the FTM application creates value on the grid side through frequency regulation and energy arbitrage. The focus of this paper is on the latter.

Most of the published work on these applications focuses on the optimal market participation of BESS. They propose optimization frameworks to create dispatch plans for charging and discharging the battery to shift energy from periods of renewable energy abundance to periods of scarcity, to optimize participation in electricity markets by buying electricity at a cheaper price and then selling it at a higher price, or to support the grid by providing balancing services. Refs. [4–6] examine the provision of frequency regulation by BESS, where the electricity market is only used for state of charge (SoC) management. Relying on a single revenue source is often insufficient to ensure profitable operation of a BESS [7], so it is important to consider multiple applications for multiple revenue streams. This justifies the development of strategies to participate in several markets simultaneously, known as multi-market or revenue stacking approaches. Refs. [3,7] propose frameworks to enable multiple applications and Refs. [8,9] suggest dispatch schemes for participation across several submarkets. Due to the 15-min intervals in the electricity market, these studies are usually carried out with step sizes no smaller than 15 min. Furthermore, a smaller step size results in a higher number of steps for a given time period, thus increasing the computational complexity of the dispatch optimization problem. However, choosing this large step size results in inaccuracies because the change in battery state between steps is not represented. This problem is particularly critical for frequency control, since the deviation of the grid frequency from its nominal value can change every second.

Numerous publications have examined the impact of degradation effects on BESS operations and dispatch optimization [10–18]. These studies on degradation-aware operation of BESS have developed more detailed simulation models of the operation and its influence on the battery state. Most of them include the resulting financial losses due to the degradation of the BESS energy capacity during operation in the objective function of the dispatch, but often simplify the dispatch by focusing on only one main application. Refs. [11–13] limit their scope to trading in the energy market with a single price signal. Ref. [18] investigates the selection of cost coefficients for degradation costs in the objective function for degradation-aware arbitrage energy trading and proposes the novel approach of optimizing revenue relative to degradation rather than simply accounting for degradation cost in the objective function by depreciation. A simple way to track degradation is to count the full equivalent cycle (FEC) during the operation of the BESS [15–17]. By relating the number counted to the expected maximum number of FECs of the battery cell, the degradation can be quantified. The degradation of the BESS can also be described by its ageing. Based on ageing, the remaining energy capacity of the BESS can be expressed in terms of the State of Health (SoH) [19]. The SoH is the ratio between the remaining energy capacity after ageing and the nominal energy capacity of the BESS. To describe the ageing of a BESS, the most common approach is to distinguish between two different ageing behaviors [14]. Static calendar ageing is caused by external effects such as temperature and time [20,21], and dynamic cycle ageing is caused by operational factors such as the number of FECs, depth of discharge (DoD) and charge rate (C-rate) [22,23]. These two ageing mechanisms can then be combined to give an overall ageing estimate. These ageing models are typically non-linear in nature and therefore difficult to incorporate into linear optimization for scheduling. In addition, the ageing models to estimate the degradation state of the BESS use lower time step sizes in the range of minutes to seconds.

This discrepancy highlights a gap between advanced dispatching models and high-resolution simulation of the condition of the BESS. Ref. [24] addresses this issue by proposing

a multi-level simulation framework in the form of a hierarchical energy management model for a hybrid BESS to bridge this gap. It includes an upper model-predictive optimization level and a lower strategy-based level that combine different timescales and modelling details. An overview of the previously discussed papers is given in Table 1. This work adopts the concept of multi-level frameworks and applies it to cross-market participation for large-scale BESS, integrating an advanced dispatch framework with a detailed ageing model.

**Table 1.** Overview of features of the proposed framework found in literature.

Literature	Region	Applications	Levels	Degradation	Time Step
[3]	Germany	FCR, ID	Optimization	Cycle counting	5 min
[4]	Germany	FCR, ID	Simulation	-	1 s
[5]	Germany	FCR	Simulation	Calendar and cycle Ageing	1 s
[6]	Nordics	FCR, DA	Optimization + Simulation	Calendar and cycle Ageing	1 h, 1 min
[7]	Germany	FCR, DA, ID	Optimization	Calendar and cycle Ageing	15 min
[8]	Nordics	FFR, FCR	Optimization	Cycle counting	1 min
[9]	Germany	aFRR, DA	Optimization	-	1 h
[11]	USA	DA, ID	Optimization	Cycle ageing	15 min
[12]	Germany	DA	Optimization	Cycle ageing	1 h
[13]	Germany	FCR, DA, ID	Optimization	Calendar and cycle ageing	15 min
[18]	Germany	ID	Optimization	Calendar and cycle ageing	15 min
[24]	Germany	ID	Optimization + Simulation	Calendar and cycle ageing	15 min, 1 min
This work	Germany	FCR, DA, ID	Optimization + Simulation	Cycle counting + calendar and cycle ageing	1 h, 15 min, 1 min

ID = Intraday trading, DA = Day-ahead trading, FCR = Provision of Frequency Containment Reserve, FFR = Provision of Fast Frequency Reserve and aFRR = automatic Frequency Restoration Reserve.

### 1.2. Paper Highlights and Structure

This work proposes a multi-level simulation framework that combines two dispatch levels with 15-min time steps and FEC-based degradation costs for day-ahead (DA) and intraday (ID) dispatch optimization, along with a simulation level that uses 1 s time steps for accurately representing the state of the BESS. This approach first optimizes and then simulates the operation and resulting revenues of a large-scale BESS for electricity market participation. To the best of the authors' knowledge, no previous studies have examined the application of large-scale BESS in multiple submarkets for energy and balancing services using cross-market optimization, including a high-resolution simulation of the resulting operation. The aim of this simulation framework is to provide a basis for evaluating operational strategies for large-scale BESS by testing them in historical market scenarios and simulating their resulting operation with a detailed model of the system. This paper lays the foundation for this research effort by providing the base simulation framework, which will be updated in the future with advanced dispatch models and improved state simulation of the BESS. The paper details the proposed framework and includes a case study illustrating the operation of a large-scale BESS. While it has been implemented for the German electricity market and its regulatory framework, it can be adapted to foreign markets by updating it according to the respective regulations. The paper is structured as follows: Section 2 provides a detailed description of the simulation framework, including its two dispatch levels and one simulation level; Section 3 presents the results of the case study; and Section 4 discusses them and provides the final conclusion of this study.

## 2. Structure of the Multi-Level Simulation Framework

The proposed simulation framework creates a digital model of a large-scale BESS, for which the use of its power and energy capacity for participation in the electricity market

is optimized. The optimized dispatch is then simulated to evaluate the resulting operation. The framework is designed to be applicable to the German electricity market, which is similar to most European countries. Participation in the German electricity markets can be realized by trading different products for specific applications and time periods. In the DA market, electric energy is sold in DA and ID auctions one day before delivery in time blocks of one hour for the former and 15 min for the latter. These short-term electricity markets are also known as spot markets. Sellers and buyers can participate in the auction by offering their individual bid and offer prices with the respective amount of energy. The final price for each production is determined at the end of the auction when supply and demand are matched. In addition, on the Continuous ID market, energy can be traded up to 5 min before delivery in hourly, 30 min and 15 min products. Bids and offers are continuously matched, resulting in dynamic price movements until the market closes. This market is mainly used to correct forecasting errors in predicting energy consumption or generation by adjusting the energy sold or bought in the previous day's auctions. These markets offer good trading opportunities for BESS due to their higher spreads, as the volatility of the energy price increases when traded closer to its delivery time [25]. For trading on the energy markets, only the DA auction and the continuous ID market with 15 min are considered, as in other studies [7,13]. This market structure of a DA and ID market fits most global energy markets with an electricity exchange [26].

The market for balancing services in Germany is mainly divided into three types [27]: frequency containment reserve (FCR) for short-term grid frequency stabilization, automatic frequency response reserve (aFRR) for frequency adjustments, and manual frequency response reserve (mFRR) for major frequency adjustments. The provision of these products is auctioned by the transmission system operator (TSO) in 4 h blocks in a power capacity auction. This results in 6 capacity products per day for each type. aFRR and mFRR have, in addition to their power capacity auction, an energy auction with 15 min products for the energy actually supplied. The capacity auction takes place one day before delivery, and the energy auction is closed on the day of delivery, 25 min before the start of the product period. The timeframes of the presented submarkets are shown in Figure 1. In the proposed simulation framework, only the provision of FCR is considered, as this is the dominant use case for large-scale BESS [2]. This results in the need to bid only for FCR capacity products, where a uniform price is derived at the end of the auction, regardless of the individual bids submitted. This method is also known as pay-as-clear. The FCR capacity products are symmetric, meaning that capacity must be offered in both positive and negative directions.

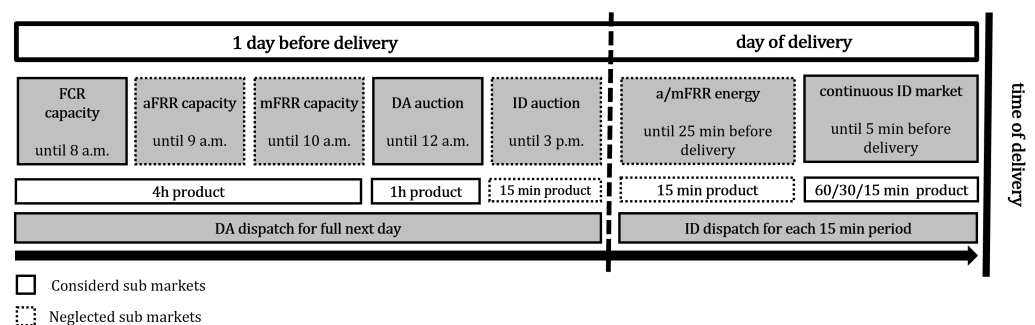


**Figure 1.** Timeframe of the submarkets in the German electricity market.

The scheduling of the operation in the proposed framework is done by two dispatch levels, as shown in Figure 2. Both are implemented as a rolling horizon by a mixed integer linear programming (MILP) optimization problem, which has to be solved. The first dispatch level is DA and represents the marketing of energy in the auctions on the day before delivery. Only the DA auction is considered, and the ID auction is neglected.

Therefore, a time step in this dispatch level has a length of 1 h, and the schedule is created for the entire following day, which serves as the control horizon for the DA dispatch level. To prevent the BESS from being completely discharged at the end of each control horizon, the two following days with their DA auction prices are used as the optimization horizon. This ensures that the BESS has enough remaining SoC at the end of the current day to optimally participate in the market by capturing the price dynamics of the following day. The second dispatch level represents trading in the continuous ID market and adjusts the bids from the previous dispatch levels for each 15-min period on the delivery day. It optimizes each 15-min time step and is re-run after each step. A higher time resolution is not relevant for the dispatch levels because the smallest product period in the German electricity market is 15 min. Therefore, smaller time steps would only increase the computational effort without improving decision-making. The resulting operating step is then simulated with a step size of 1 s, including the realized FCR calls caused by the frequency deviation by the simulation level of the framework. The final state of the BESS in the simulated step is the initial state of the next optimization step. This loop through the ID dispatch and simulation levels is repeated for each 15-min timeframe of the day and then repeated with the next schedule from the DA dispatch level for the next day. The next day's DA prices are also included in the ID optimization for the same reason as in the DA optimization above. This adequately reflects the real market environment by separating the DA and ID decision-making. The dynamic price fluctuation in the continuous ID market for the same 15-min product, caused by the continuous matching of buy and sell orders, is ignored for simplicity. In general, perfect price forecasting is assumed for all price signals, and the price forecasting error is neglected for simplicity. This assumption leads to an overestimation of revenue, and the use of a forecasted price signal will reduce the simulated revenue. Thereby, a higher energy capacity for the same power capacity results in a higher sensitivity to the accuracy of the price forecast [28]. The proposed simulation framework is shown in Figure 3. Due to its market dominance, lithium technology has been considered for the BESS in this work [2]. Each level of the framework is described in detail in the following subchapters. The simulation framework is implemented in Python 3.12.7 [29], where the optimization problems of the two dispatch levels are constructed using Pyomo 6.8.0 [30] and solved using Gurobi 11.0.0 [31]. The basic modelling of the BESS is derived and extended from a previously published work [32].

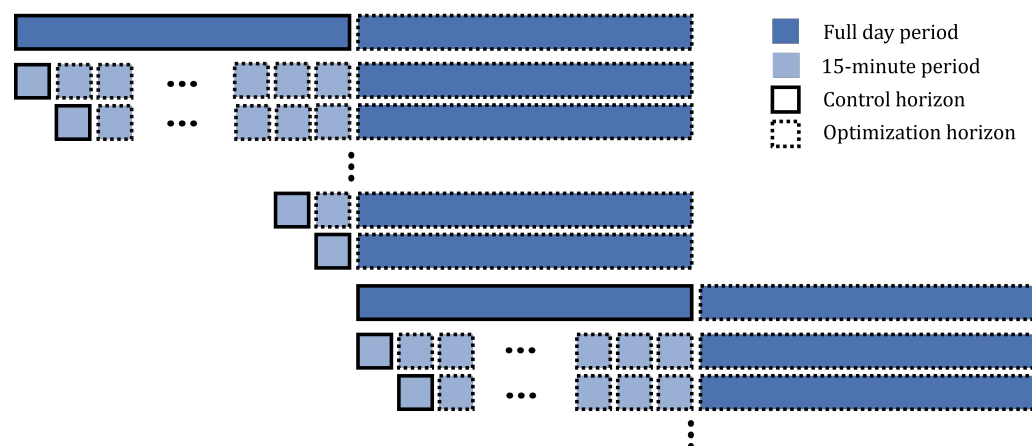


**Figure 2.** Sequence of optimization steps in the two dispatch levels.

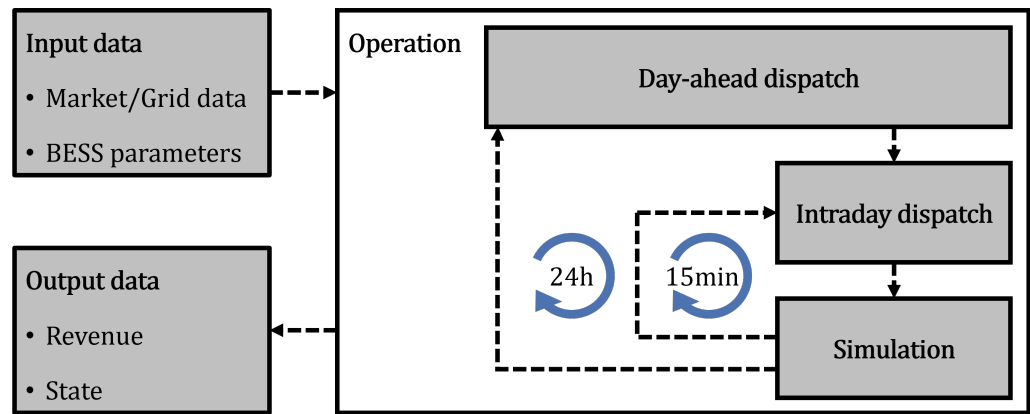


**Figure 3.** Structure of the proposed simulation framework with two dispatch levels and one simulation level.

### 2.1. Day-Ahead Dispatch Level

The DA dispatch level of the framework is based on MILP, which creates an optimization problem with a specifically defined objective function to be maximized. This problem has to be solved by the solver to derive the optimal schedule for the BESS. The objective function  $F_{DA}$  of the DA optimization is to maximize the revenue generated by the DA dispatch. The total revenue of the DA dispatch is derived from the revenue from participating in the DA auction, the revenue from the FCR capacity auction, and the losses due to the degradation of the battery when following the schedule, which is shown in Equation (1). The DA auction revenue is calculated from the marketed power  $P_{DA}$ , the length of a time step  $\Delta t$ , and the energy price  $c_{DA}$ . The FCR revenue is derived from the marketed capacity  $C_{FCR}$  and the capacity price  $c_{FCR}$ . The degradation costs are derived from the number of full equivalent cycles  $\Delta FEC$  of the battery and the cycle cost  $c_{FEC}$ . This cost-based inclusion of degradation in the objective function is common for degradation-aware operation of BESS [13,14].

$$\text{Max } F_{DA} = \sum_t [P_{DA}(t) \cdot \Delta t \cdot c_{DA}(t) + C_{FCR}(t) \cdot c_{FCR}(t) - \Delta FEC(t) \cdot c_{FEC}] \quad (1)$$

To ensure the desired operating behaviour, the objective is maximized according to constraints. These define the relationships between variables and parameters, thereby creating the model equations. Boundary conditions for the operation of the BESS can also be defined. The SoC of the BESS is derived from the SoC of the previous step, the charge power  $P_{charge}$ , the discharge power  $P_{discharge}$ , the efficiency  $\eta$ , SoH and the nominal energy capacity  $E_n$  of the BESS, as shown in Equation (2). The SoH used in this calculation is treated as a static parameter at the dispatch level. For each day of the simulation, the final SoH value obtained from the ageing model of the simulation level (as discussed in Section 2.3) from the previous day is taken. The initial SoH value for the first day of the simulation period is predefined.

$$\text{SoC}(t) = \text{SoC}(t-1) + \frac{[P_{charge}(t-1) \cdot \eta - P_{discharge}(t-1)/\eta] \cdot \Delta t}{\text{SoH} \cdot E_n} \quad (2)$$

The power planned in the DA auction is divided into charge and discharge power by Equation (3), while Equation (4) ensures that the power does not exceed the power capacity of the BESS.  $u_{discharge}$  and  $u_{charge}$  are binary state variables for discharge and

charge operation, which, along with with Equation (5), ensures that the battery is not simultaneously charged and discharged.

$$P_{\text{discharge}}(t) - P_{\text{charge}}(t) = P_{\text{DA}}(t) \quad (3)$$

$$0 \leq P_k(t) \leq P_n \cdot u_k, \quad \forall k \in \{\text{charge, discharge}\} \quad (4)$$

$$u_{\text{discharge}}(t) + u_{\text{charge}}(t) \leq 1 \quad (5)$$

When marketing the capacity of BESS in the FCR auction under the regulatory framework [33], the nominal power capacity must exceed the marketed capacity by at least 25%. This results in the requirement that the capacity offered may not exceed 80% of the nominal power capacity of BESS, enforced by Equation (6). Furthermore, the capacity is offered for a period of 4 h; therefore, the capacity for FCR must be constant for this period (Equation (7)). Equation (8) ensures that the sum of the offered FCR capacity and the remaining capacity for marketing on the spot markets  $C_{\text{spot}}$  does not exceed the nominal power capacity of the BESS. Furthermore, Equation (9) keeps  $P_{\text{DA}}$  within the previously mentioned capacity limits for spot market trading.

$$C_{\text{FCR}}(t) \leq P_n \cdot 0.8 \quad (6)$$

$$C_{\text{FCR}}(t) = C_{\text{FCR}}(t+1) \quad \forall j \in \{0, 1, \dots, 5\}, \quad \forall t \in \{4j, 4j+1, 4j+2\} \quad (7)$$

$$C_{\text{FCR}}(t) + C_{\text{spot}}(t) \leq P_n \quad (8)$$

$$-C_{\text{spot}}(t) \leq P_{\text{DA}}(t) \leq C_{\text{spot}}(t) \quad (9)$$

In addition, Equations (10) and (11) also ensure that the regulatory limits for SoC are maintained during the operation of the storage system. This ensures that the BESS can always provide its offered power capacity for FCR in both positive and negative directions for a minimum period of 15 min.

$$\text{SoC}(t) \leq \frac{\text{SoH}(t) \cdot E_n - C_{\text{FCR}}(t) \cdot 15 \text{ min}}{\text{SoH}(t) \cdot E_n} \quad (10)$$

$$\text{SoC}(t) \geq \frac{C_{\text{FCR}}(t) \cdot 15 \text{ min}}{\text{SoH}(t) \cdot E_n} \quad (11)$$

To assess the degradation cost of the battery during its operation, the  $\Delta\text{FEC}$  for each time step is calculated from the charging/discharging power and the nominal energy capacity of the BESS in Equation (12). Since the resulting FCR activation calls, depending on the grid frequency deviation, cannot be predicted, a term for the average used FEC per FCR capacity during a time step  $\text{FEC}_{\text{FCR}}$  multiplied with  $C_{\text{FCR}}$  is added. This value is derived from the frequency data of the simulated period, and the resulting distribution is shown in Figure 4. The respective expected degradation costs per FEC are calculated from the specific cost of the BESS  $c_{\text{BESS}}$ , the expected number of FEC of the battery cells  $\text{FEC}_{\text{EoL}}$  until the end of life (EoL), and  $E_n$ , as shown in Equation (13).

$$\Delta\text{FEC}(t) = \frac{[P_{\text{charge}}(t) + P_{\text{discharge}}(t)] \cdot \Delta t}{2 \cdot E_n} + \text{FEC}_{\text{FCR}} \cdot C_{\text{FCR}} \quad (12)$$

$$c_{\text{FEC}} = \frac{c_{\text{BESS}} \cdot E_n}{\text{FEC}_{\text{EoL}}} \quad (13)$$

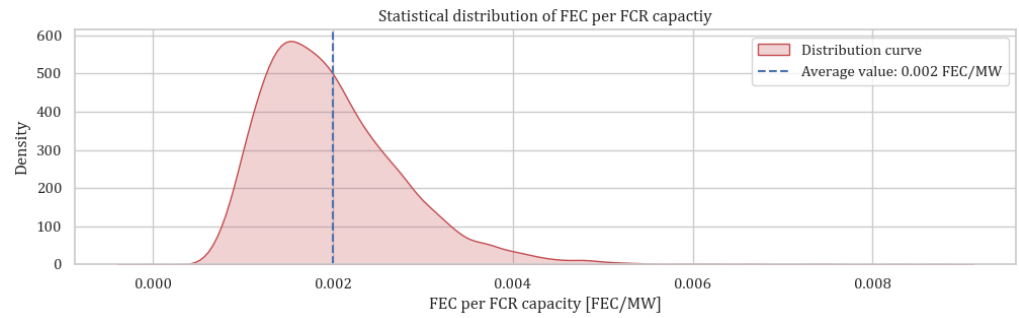


**Figure 4.** Distribution of FEC per FCR capacity during one-hour time periods based on the frequency data of the simulated period.

## 2.2. Intraday Dispatch Level

Upon completion of the DA dispatch optimization, the BESS operation plan will be re-optimized ID. This will respect the DA schedule for FCR and DA market participation. The ID trading and SoC management of the BESS during the provision of FCR is managed by buying and selling energy on the continuous ID market. Each 15-min period of the day is optimized, using the rest of the day and the next day as the optimization horizon. The objective function for the ID dispatch  $F_{ID}$  is the revenue generated by trading on the continuous ID market and is therefore given by Equation (14) by the marketed power  $P_{ID}$  and the corresponding prices  $c_{ID}$  on the ID market, the cycle costs, and an added penalty  $V_{penalty}$  with its weight  $w_{penalty}$ . This penalty term helps the ID dispatch to stay within the SoC bounds by penalizing operations close to the FCR reserve. Without this term, the SoC could drift outside the SoC bounds while simulating second-by-second FCR calls, which is not allowed.

$$\text{Max } F_{ID} = \sum_t [P_{ID}(t) \cdot \Delta t \cdot c_{ID}(t) - \Delta FEC(t) \cdot c_{FEC} + V_{penalty}(t) \cdot w_{penalty}] \quad (14)$$

Since the power marketed in the DA dispatch must be respected, the schedule created there is considered a fixed operation plan. The optimization adjusts this schedule with its marketed power on the continuous ID market. The realized power is therefore a superposition of DA and ID scheduled power, resulting in the power balance shown in Equation (15). Furthermore, the ID dispatch must ensure that the adjusted power schedule is within the power capacity reserved for spot market trading (Equation (16)).

$$P_{discharge}(t) - P_{charge}(t) = P_{DA}(t) + P_{ID}(t) \quad (15)$$

$$-C_{spot}(t) \leq P_{DA}(t) + P_{ID}(t) \leq C_{spot}(t) \quad (16)$$

Due to the unpredictability of the grid frequency deviation, the activation calls to provide the FCR cannot be sufficiently predicted. Therefore, these calls cannot be anticipated in the ID dispatch optimization. Therefore, the SoC limits are updated, and a SoC penalty band is included (Figure 5), scaled by the above-mentioned penalty value. This penalty-based SoC management automatically drifts the SoC away from the FCR reserve and represents a more dynamic SoC recovery strategy than the static ones used in the literature [4,6]. The formulation of the updated SoC limits is shown in Equations (17) and (18).

$$SoC(t) \leq \frac{SoH(t) \cdot E_n - C_{FCR}(t) \cdot (1 + V_{penalty}(t)) \cdot 15 \text{ min}}{SoH(t) \cdot E_n} \quad (17)$$

$$SoC(t) \geq \frac{C_{FCR}(t) \cdot (1 + V_{penalty}(t)) \cdot 15 \text{ min}}{SoH(t) \cdot E_n} \quad (18)$$

The state of charge definition from Equation (2), the charging and discharging power modelling from Equations (4) and (5), the degradation cost modelling from Equations (12) and (13) are taken from the DA dispatch level and implemented in the same way in ID dispatch.

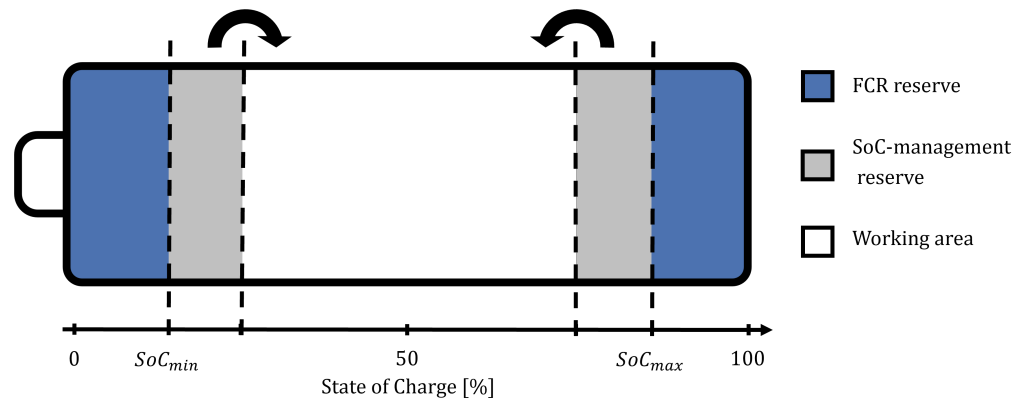


**Figure 5.** Energy capacity reserved for FCR and SoC-management.

### 2.3. Simulation Level

The simulation level of the framework does not include any optimization like the previous dispatch levels. It simply takes the specific input values and calculates the corresponding output values of the system based on the model functions. This level of the framework takes the 15-min control step from the ID dispatch and simulates the resulting SoC in 1-s steps, including the FCR calls caused by grid frequency deviation. The final SoC value is then used as the start value for the next ID dispatch iteration. The activated power for FCR  $P_{FCR}$  is derived according to the grid regulation [33] as shown in Equation (19) from the marketed FCR capacity and the deviation of the grid frequency  $\Delta f$  from its nominal value of 50 Hz.

$$P_{FCR}(t) = \begin{cases} C_{FCR}(t), & \forall \Delta f > 0.2 \text{ Hz} \\ C_{FCR}(t) \cdot \frac{\Delta f(t)}{0.2 \text{ Hz}}, & \forall 0.01 \text{ Hz} \leq |\Delta f| \leq 0.2 \text{ Hz} \\ 0, & \forall |\Delta f| \leq 0.01 \text{ Hz} \\ -C_{FCR}(t), & \forall \Delta f < -0.2 \text{ Hz} \end{cases} \quad (19)$$

The charging and discharging of the battery for each second is derived from the DA and ID power plus the activated FCR power according to Equation (20).

$$P_{\text{discharge}}(t) - P_{\text{charge}}(t) = P_{DA}(t) + P_{ID}(t) + P_{FCR}(t) \quad (20)$$

The SoC of the battery is calculated in the same way as in the previous two stages, using Equation (2). In order to quantify the degradation of the energy capacity for the simulated operation, an ageing model is included in the simulation level, which is used to derive the change in state of health of the battery. The ageing model is taken from [20,22], where the modelling is derived by fitting model parameters to real tests of LFP battery cells and validated for dynamic conditions. To compare the SoH-based degradation with the FEC-based degradation, the number of FECs of the resulting operation is counted as in the two dispatch levels. For both degradation models, the resulting degradation costs are calculated and compared. This is done to justify the use of FEC counting to address degradation in the dispatch levels and will be discussed in more detail in Section 3.1. As mentioned above, the ageing of the BESS can be divided into static calendar ageing and dynamic cycle ageing. The resulting total ageing  $Q_{\text{age}}^{\text{total}}$  is the superposition of both the

calendar ageing  $Q_{\text{age}}^{\text{cal}}$  and the cycle ageing  $Q_{\text{age}}^{\text{cyc}}$ , as shown in Equation (21). Based on the total ageing during a time step and the  $SoH$  of the previous time step, the resulting  $SoH$  for the current time step can be calculated by Equation (22).

$$Q_{\text{age}}^{\text{total}}(t) = Q_{\text{age}}^{\text{cal}}(t) + Q_{\text{age}}^{\text{cyc}}(t) \quad (21)$$

$$SoH(t) = SoH(t-1) - Q_{\text{age}}^{\text{total}}(t) \quad (22)$$

Calendar ageing can be expressed as a function of temperature  $T$ , SoC, and time  $\Delta t$  with the temperature-dependent factor  $k_T$  and the SoC dependent factor  $k_{SoC}$  (Equation (23)). Cycle ageing is calculated from  $T$ ,  $C - rate$ ,  $DoD$ , and  $\Delta FEC$ , with the  $k_T$ , the C-rate-dependent factor  $k_{C-rate}$ , and the DoD-dependent factor  $k_{DoD}$  (Equation (24)). The factors used are described and derived in detail in [20,22] with their fitting parameters. To simplify the simulation model, ideal cooling is assumed. This leads to a constant battery temperature and results in  $k_T = 1$ .

$$Q_{\text{age}}^{\text{cal}}(T, SoC, \Delta t) = k_T(T) \cdot k_{SoC}(SoC) \cdot \sqrt{\Delta t} \quad (23)$$

$$Q_{\text{age}}^{\text{cyc}}(T, C - rate, DoD) = k_T(T) \cdot k_{C-rate}(C - rate) \cdot k_{DoD}(DoD) \cdot \sqrt{\Delta FEC} \quad (24)$$

As the current ageing of the battery is highly dependent on the previous ageing, the concept of virtual time  $t^*$  and cycles  $FEC^*$  is introduced. The total ageing of the battery in the previous step is reformulated into a time span and a number of FECs, which are needed to achieve the same ageing with the current battery conditions by Equations (25) and (26).

$$t^* = \left( \frac{Q_{\text{age}}^{\text{total}}(t-1)}{k_T \cdot k_{SoC}} \right)^2 \quad (25)$$

$$FEC^* = \left( \frac{Q_{\text{age}}^{\text{total}}}{k_T \cdot k_{C-rate} \cdot k_{DoD}} \right)^2 \quad (26)$$

The current calendar and cycle ageing can then be calculated by linearizing around the current battery conditions, as shown in Equations (27) and (28). Due to the mathematical formulation of the ageing model, an initial ageing of 0% cannot be calculated. It is therefore assumed that the initial ageing of the BESS is 1% and therefore the  $SoH_{\text{init}}$  is 99%.

$$Q_{\text{age}}^{\text{cal}}(t) = \frac{dQ_{\text{age}}^{\text{cal}}(\Delta t)}{d\Delta t} \cdot \Delta t = \frac{k_T \cdot k_{SoC}}{2 \cdot \sqrt{t^*}} \cdot \Delta t \quad (27)$$

$$Q_{\text{age}}^{\text{cyc}}(t) = \frac{dQ_{\text{age}}^{\text{cyc}}(\Delta FEC)}{d\Delta FEC} \cdot \Delta FEC(t) = \frac{k_T \cdot k_{C-rate} \cdot k_{DoD}}{2 \cdot \sqrt{FEC^*}} \cdot \Delta FEC(t) \quad (28)$$

Based on the two degradation values,  $\Delta FEC$  and  $Q_{\text{age}}^{\text{total}}$ , two different degradation cost functions can be derived [14]. The first is the SoH-based degradation cost  $c_{\text{SoH}}^{\text{deg}}$  shown in Equation (29), and the second is the SoH-based degradation cost calculated in Equation (30) based on the BESS EoL criteria  $SoH_{\text{EoL}}$  with the typical value of 80 % [14]. The FEC-based ageing costs  $c_{\text{FEC}}^{\text{deg}}$  used in the dispatch levels are also implemented at the simulation level to calculate the final degradation cost of the resulting operation.

$$c_{\text{SoH}}^{\text{deg}} = \frac{c_{\text{BESS}} \cdot E_n}{1 - SoH_{\text{EoL}}} \cdot Q_{\text{age}}^{\text{total}}(t) \quad (29)$$

$$c_{\text{FEC}}^{\text{deg}} = c_{\text{FEC}} \cdot \Delta FEC(t) \quad (30)$$

#### 2.4. Input Data for the Chase Study

The simulation framework uses input data for the full year 2024, which captures annual seasonality and improves the generalizability of the results. The settlement prices in the capacity auction for FCR during the period considered are taken from the website of the German TSO [34], where the auction takes place and the results of each auction are published. Prices from the DA auction for the DA dispatch level and from the continued ID market for the ID dispatch level are taken from the website of EPEX Spot [35], the largest electricity exchange for the German market. Clearing prices are used for the DA auction. As the price for a specific one-hour period product is derived after the closing time, the prices provided are indeed tradable. For the continuous ID market, prices from the ID1 index are used due to the dynamic price development. These are the weighted average prices of the 15 min period products up to market close. The spreads in these index prices are lower than the possible spreads in the dynamic price development of the continuous ID market. This results in rather conservative revenue approximations for trading in this submarket, which are sufficient for this work. The grid frequency data for the period used are taken from the German TSO's website "netztransparenz.de" [36]. The parameter for the BESS model are summarized in Table 2. A power-to-capacity ratio of 1/2 is used because it reflects current market trends [2].

**Table 2.** Parameter used in the modeling of the BESS.

Parameter	Value
$P_n$	10 MW
$E_n$	20 MWh
$\eta$	90%
$c_{\text{BESS}}$	380,000 €/MWh [2]
$FEC_{\text{EoL}}$	3500 FEC [37]
$SoH_{\text{EoL}}$	80% [14]
$FEC_{\text{FCR}}$	0.002 FEC/MW

### 3. Results

The presented simulation framework generates two dispatch levels, one for the DA auction and one for the continuous ID market. The DA plans are updated with the ID plan, resulting in a final operational plan. The realized operation according to these levels is then simulated second by second in the simulation level of the framework. The resulting total revenue from the simulated operation of the BESS over the entire simulation period of the year 2024 and its revenue components are shown in Table 3. Overall, the FCR market generates the most revenue, followed by the DA market. It should be noted that the cost of charging the BESS to stay in the required working area for the provision of FCR is included in the ID revenue. Therefore, the even if the ID revenue is the lowest revenue source, this market is still very important for cross-market participation. While both FEC-based and SoH-based degradation models provide insights into BESS degradation, the FEC-based model offers greater consistency because it is independent of the initial states of health. Therefore, FEC-based degradation cost is used to calculate the final cost of the resulting operation. This decision is discussed in detail in Section 3.2. After considering the degradation costs, the simulated operation of the BESS is still profitable, with a total revenue of €1 million.

The revenue of each month in the simulated period is shown in Figure 6. It shows a high seasonal variation of revenues, with higher revenues in summer and lower revenues in winter. The lowest monthly revenue is achieved in February, with a revenue of 30,000 EUR, while the highest monthly revenue is achieved in June, with almost

200,000 EUR. The monthly revenues show that the FCR revenue is more stable over the period of one year in comparison to the DA and ID revenue. The simulated revenue of the large-scale BESS for the studied time period is in the same range as the assumed revenue potential of such a system in the German market provided by a transparent index [38], where the yearly revenue generated through the provision for FCR alone varies between 50,000 and 120,000 EUR per 1 MW installed power capacity, validating the simulation results. The simulation framework was run on a Windows 11 machine with an Intel Core i9-10885h CPU at 2.40 GHz and 32 GB of RAM, and the optimization and simulation of the example year 2024 take 4 to 5 h.

**Table 3.** Revenue components of the simulated operation for the entire simulation period.

Revenue Component	Revenue
FCR	1,114,370.71 €
Day-ahead	230,006.18 €
Intraday	110,104.58 €
Degradation	−379,970.42 €
Total	1,074,511.05 €

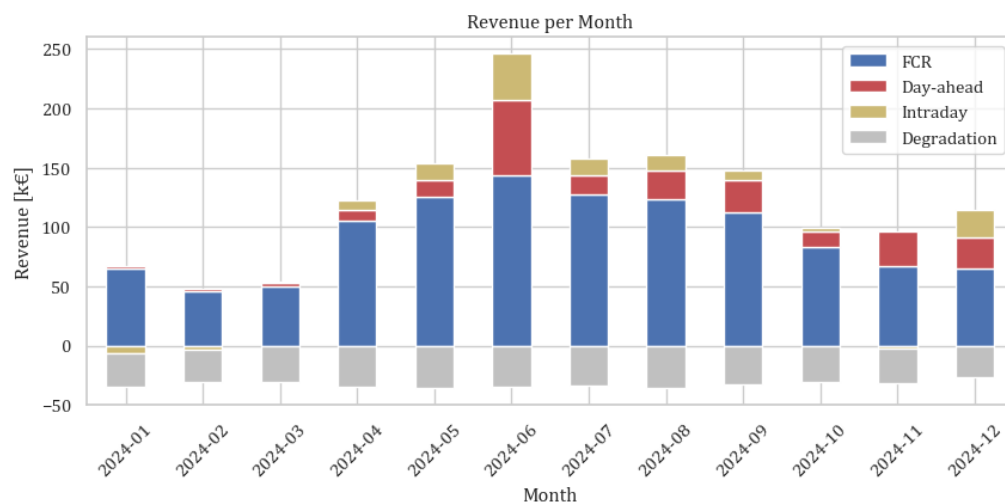


**Figure 6.** Resulting revenue per month of the simulated period.

### 3.1. Resulting Dispatch and Operation

The optimized dispatch plan and the resulting operation for the example period of June 15th to 19th is shown in Figure 7 with their underlying price signals. The lowest graph in the figure shows the capacity allocation. It shows that the majority of the BESS capacity is reserved for the provision of FCR due to its high profitability. The graph above shows the three price signals for that period. It can be seen that the price of the continuous ID market correlates with the DA auction price most of the time but fluctuates around the DA price. This is due to the structure of these two markets and their use case, where the continuous ID market is used to adjust the marketed energy in the DA auction. The FCR capacity price is decoupled from the other two spot market prices because it is a product from a different submarket, and therefore the relationship of this price signal to the other two spot market signals is not easily visible. The second chart from the top shows the DA and ID energy dispatch schedules. The ID dispatch is much more active due to its smaller step size and its task to manage the BESS SoC for FCR provisioning. The utilization of the local price minima and maxima can be seen from the peaks in the intraday power profile. It can also be seen that the two schedules are opposite at some time steps, where energy is sold on the DA

market and then bought back for the same period on the continuous ID market, or vice versa. This is a viable strategy when the price on the continuous ID market deviates from the price on the DA auction and a pure financial trade can be realized. This results in the mutual neutralization of both orders, and there is no need to load or unload the BESS. This operation is attractive because it can generate revenue without a realized BESS operation, and therefore no degradation effects, making it highly profitable. However, this type of market participation is not easily predictable. Therefore, these trades can only be realized spontaneously when the market development in the continuous ID market opens up these opportunities. The upper diagram shows the realized power profile of the BESS for the example period and the resulting SoC. This simulation can therefore be used to verify that the operational limits of the FCR rule are met and that the resulting operation is valid under the regulatory framework. The presentation of the operation results of the three levels of the simulation framework shows how complex the dispatch and operation of a relatively simple energy asset like a BESS can be. This operational behaviour cannot be adequately represented by simple optimization with one single optimization. This underlines the importance of such advanced simulation frameworks as presented in this work.

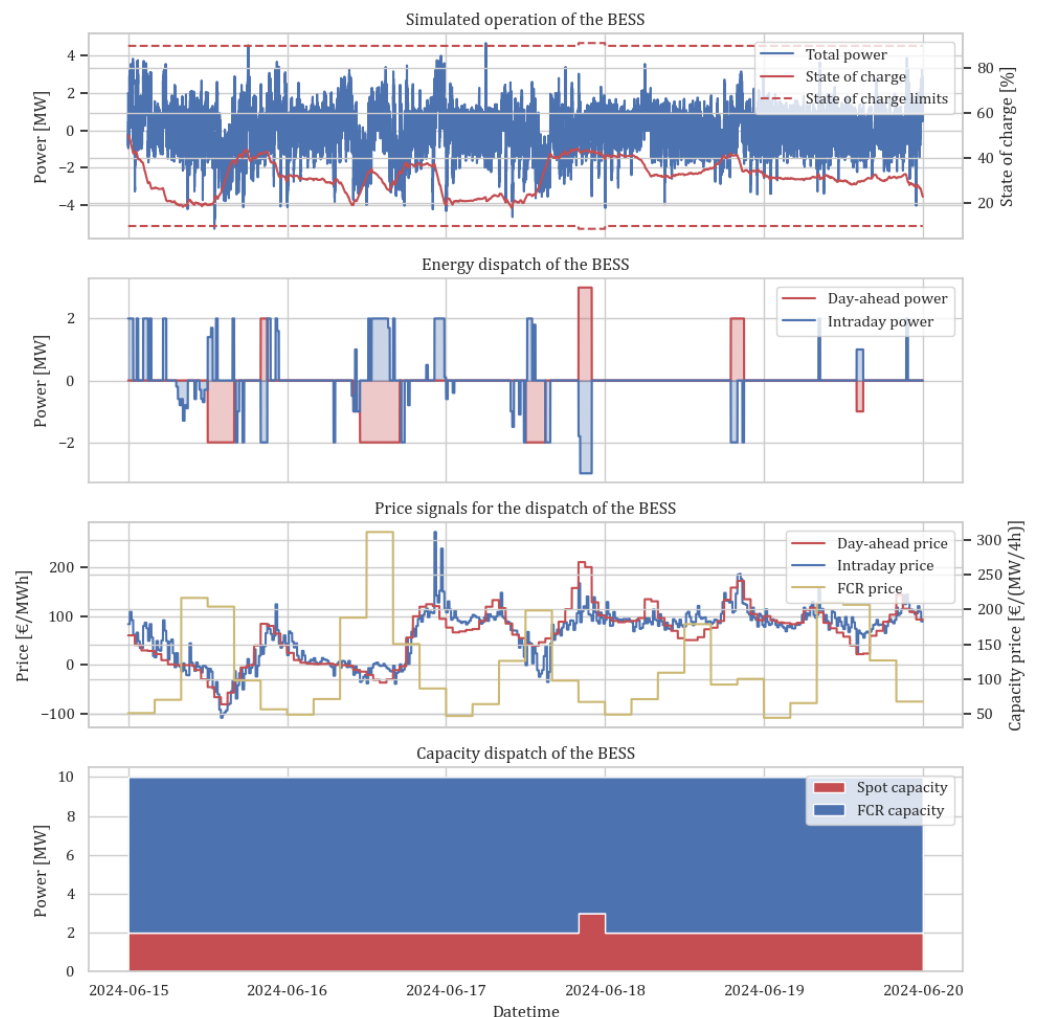


**Figure 7.** Resulting dispatch and simulated operation of the BESS for the exemplary date of June 15th to 19th. The top plot shows the simulated operation. The second plot presents the DA and ID dispatch for spot market trading. The third plot displays the price signals used for dispatch decisions. The bottom plot shows the capacity allocation between the spot and FCR markets.

### 3.2. Degradation Costs

The resulting degradation of the BESS by the operation and the resulting cost are shown in Table 4. There, the resulting FEC-based degradation is shown, as well as the results from the SoH-based model with different initial SoH to show their impact on the degradation estimation of the BESS. With an initial SoH of 99%, the degradation is relatively high and would lead to an unprofitable operation of the BESS in the simulated period by including the SoH-based degradation cost. Using these degradation costs to make dispatch decisions may underutilize the BESS and result in lower revenue, as discussed in [18]. The SoH-based costs with an initial SoH of 95 and 90% are closer to the calculated costs of the FEC-based degradation model. Figure 8 shows the cumulation of degradation costs over the simulated time period. The typical square root shape of the calendar ageing can be seen in the SoH-based degradation cost with an initial SoH of 99%. The other modelled degradation costs have a more linear shape compared to the former mentioned. The initial higher ageing at the beginning of the battery life is due to the growth of the solid electrolyte interphase [39,40]. This mechanism slows down at a SoH of 95% where the ageing process becomes more stable. SoH-based costs vary significantly depending on the initial SoH and have a more non-linear behaviour at higher SoH levels. This would result in different dispatch decisions for different degradation states of the BESS when using SoH-based degradation cost in the dispatch optimization, leading to uncertainty in economic projections. To study the impact of SoH-based degradation cost in the dispatch levels, the cycle cost from Equation (13) is exchanged with the following ageing-based cycle cost (Equation (31)), derived from the introduced ageing model. Thereby, the linearized cycle ageing term is used for the current BESS conditions.

$$c_{\text{FEC}} = \frac{c_{\text{BESS}} \cdot E_n}{1 - \text{SoH}_{\text{EoL}}} \cdot \frac{dQ_{\text{age}}^{\text{cyc}}(\Delta\text{FEC})}{d\Delta\text{FEC}} \quad (31)$$

By replacing the static degradation costs in the dispatch with more dynamic SoH-based costs from Equation (31) and repeating the simulation study with an initial SoH of 99%, the previously mentioned assumptions can be underlined. The resulting dispatch not only underutilizes the BESS; it actually leads to the idle state of the system because every action causes high degradation costs, and therefore the solver cannot find a profitable operation plan. It shows that the more detailed degradation information used at the dispatch level leads to an extremely unprofitable and therefore undesirable operation. Consequently, the simple counting of FECs is the better choice for estimating the degradation cost during dispatch decision-making in this study. This underlines the complexity of degradation-aware operation and how degradation costs should be considered in dispatch decisions. Rather than implementing complex dispatch models with nonlinearities to accurately represent ageing behaviour; the idea of optimizing revenue per unit degradation from [18] can be taken up and implemented by optimizing revenue per FEC of BESS in future work.

**Table 4.** Degradation and the resulting costs for the different degradation models.

Degradation Model	Degradation Value	Degradation Cost
FEC-based	174.98 FEC	379,970.42 €
SoH-based ( $\text{SoH}_{\text{init}} = 99\%$ )	3.12%	1,186,015.03 €
SoH-based ( $\text{SoH}_{\text{init}} = 95\%$ )	1.40%	532,694.61 €
SoH-based ( $\text{SoH}_{\text{init}} = 90\%$ )	0.77%	292,432.41 €

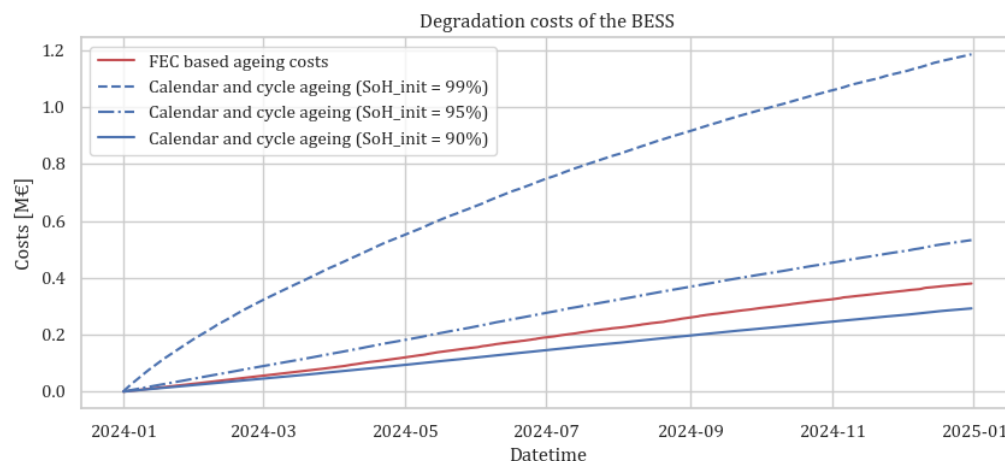


**Figure 8.** Cumulative degradation costs of different models over the simulated time period.

#### 4. Discussion and Conclusions

This study presents a multi-level simulation framework integrating cross-market optimization with degradation-aware dispatching for large-scale BESS. By adequately representing the structure of the electricity market through the differentiation between DA and ID dispatching, the optimization model can be transferred to real-life application. While optimizing market participation in the FCR, DA, and ID markets, the resulting operation is simulated and the degradation is quantified. To validate the framework, a simulation study of market participation in the German electricity market for the year 2024 is performed. The FCR market remains the main source of revenue, followed by the DA and ID markets. However, the ID market plays a crucial role in managing SoC and ID adjustments, which ultimately contributes to overall profitability. The comparison between FEC-based and SoH-based degradation models highlights the complexity of accurately estimating degradation costs. While SoH-based methods provide a detailed representation of degradation, they introduce variability based on initial degradation conditions, making FEC-based cost estimation a more practical choice for dispatch-level optimization. Nevertheless, a SoH-based ageing model is much more accurate and should still be preferred for in-depth ageing simulation. While the framework provides a robust basis for optimizing and simulating large-scale BESS operations, some limitations should be addressed in future research. The simulation could be extended to represent the full lifetime of the BESS. This can be done by assuming constant price levels and volatility, and repeating the results for the year simulated in this work until the EoL of the BESS, as shown in [18]. The assumption of constant temperature due to perfect cooling can be dropped, and a thermal model with accurate representation of cooling and efficiency can be incorporated. This allows a more realistic simulation model for a BESS to be formulated, resulting in a more realistic ageing simulation. Furthermore, the assumption of perfect price forecasting simplifies the optimization problem but does not reflect real-world uncertainties. Future work should include price forecasting to show the impact of forecasting errors on the operation and its financial consequences. This will provide an opportunity to explore how uncertainties can be addressed in the dispatch decision. This extension will make the simulation results more realistic and comparable to real-world implementations. In addition, extending the framework to include additional revenue streams, such as aFRR and mFRR, could further optimize and stabilize BESS profitability.

**Author Contributions:** Conceptualization, L.T.; Methodology, L.T.; Validation, L.T.; Investigation, L.T.; Data curation, L.T.; Writing—original draft, L.T.; Writing—review & editing, L.T. and G.F.; Supervision, G.F. All authors have read and agreed to the published version of the manuscript.

**Funding:** This research received no external funding.

**Data Availability Statement:** The original contributions presented in the study are included in the article, further inquiries can be directed to the corresponding author.

**Conflicts of Interest:** The authors declare no conflict of interest.

## Abbreviations

The following abbreviations and nomenclature are used in this manuscript:

### Abbreviations

aFRR	automatic Frequency Restoration Reserve
BESS	Battery Energy Storage System
BTM	Behind the Meter
C-rate	Charge rate
DA	Day-ahead
DoD	Depth of Discharge
EoL	End of Life
FCR	Frequency Containment Reserve
FEC	Full Equivalent Cycle
FTM	Front of the Meter
ID	Intraday
mFRR	manual Frequency Restoration Reserve
MILP	Mixed Integer Linear Programming
SoC	State of Charge
SoH	State of Health
TSO	Transmission System Operator

### Nomenclature

$\Delta FEC$	Change in number of FECs [-]
$\Delta t$	Time step duration [h]
$\eta$	Efficiency of the battery system [%]
$c_{DA}$	Day-ahead price [€/MWh]
$c_{ID}$	Intraday price [€/MWh]
$C_{FCR}$	FCR capacity [MW]
$c_{FCR}$	FCR price coefficient [€/ (MW/h)]
$c_{FEC}$	Degradation cost per FEC [€]
$C_{spot}$	Spot market capacity [-]
$E_n$	Nominal energy capacity [MWh]
$P_{charge}$	Charging power [MW]
$P_{DA}$	Day-ahead power [MW]
$P_{ID}$	Intraday power [MW]
$P_{discharge}$	Discharging power [MW]
$P_{FCR}$	Activated FCR power [MW]
$P_n$	Nominal power capacity [MW]
SoC	State of Charge [%]
SoH	State of Health of the battery [%]
$u_{charge}$	Binary charging state [-]
$u_{discharge}$	Binary discharging state [-]
$V_{penalty}$	Penalty term [-]
$w_{penalty}$	Weight for penalty term [-]

## References

1. International Energy Agency (IEA). Batteries and Secure Energy Transitions. Available online: <https://www.iea.org/reports/batteries-and-secure-energy-transitions> (accessed on 17 March 2025).
2. Figgenger, J.; Hecht, C.; Haberschusz, D.; Bors, J.; Spreuer, K.G.; Kairies, K.P.; Stenzel, P.; Sauer, D.U. The development of battery storage systems in Germany: A market review (status 2023). *arXiv* **2022**, arXiv:2203.06762.
3. Englberger, S.; Jossen, A.; Hesse, H. Unlocking the potential of battery storage with the dynamic stacking of multiple applications. *Cell Rep. Phys. Sci.* **2020**, *1*, 100238. [[CrossRef](#)]
4. Thien, T.; Schweer, D.; vom Stein, D.; Moser, A.; Sauer, D.U. Real-world operating strategy and sensitivity analysis of frequency containment reserve provision with battery energy storage systems in the german market. *J. Energy Storage* **2017**, *13*, 143–163. [[CrossRef](#)]
5. Fleeer, J.; Zurmühlen, S.; Meyer, J.; Badeda, J.; Stenzel, P.; Hake, J.F.; Sauer, D.U. Price development and bidding strategies for battery energy storage systems on the primary control reserve market. *Energy Procedia* **2017**, *135*, 143–157. [[CrossRef](#)]
6. Astero, P.; Evens, C. Optimum operation of battery storage system in frequency containment reserves markets. *IEEE Trans. Smart Grid* **2020**, *11*, 4906–4915. [[CrossRef](#)]
7. Braeuer, F.; Rominger, J.; McKenna, R.; Fichtner, W. Battery storage systems: An economic model-based analysis of parallel revenue streams and general implications for industry. *Appl. Energy* **2019**, *239*, 1424–1440. [[CrossRef](#)]
8. Casla, I.M.; Khodadadi, A.; Söder, L. Optimal day ahead planning and bidding strategy of battery storage unit participating in nordic frequency markets. *IEEE Access* **2022**, *10*, 76870–76883. [[CrossRef](#)]
9. Nitsch, F.; Deissenroth-Uhrig, M.; Schimeczek, C.; Bertsch, V. Economic evaluation of battery storage systems bidding on day-ahead and automatic frequency restoration reserves markets. *Appl. Energy* **2021**, *298*, 117267. [[CrossRef](#)]
10. Zhang, L.; Yu, Y.; Li, B.; Qian, X.; Zhang, S.; Wang, X.; Zhang, X.; Chen, M. Improved cycle aging cost model for battery energy storage systems considering more accurate battery life degradation. *IEEE Access* **2021**, *10*, 297–307. [[CrossRef](#)]
11. Singh, A.; Pareek, P.; Sampath, L.P.M.I.; Goel, L.; Gooi, H.B.; Nguyen, H.D. A Stress-Cognizant Optimal Battery Dispatch Framework for Multimarket Participation. *IEEE Trans. Ind. Inform.* **2024**, *20*, 7259–7268. [[CrossRef](#)]
12. Keske, C.; Srinivasan, A.; Sansavini, G.; Gabrielli, P. Optimal economic and environmental arbitrage of grid-scale batteries with a degradation-aware model. *Energy Convers. Manag. X* **2024**, *22*, 100554. [[CrossRef](#)]
13. Hesse, H.C.; Kumtepelı, V.; Schimpe, M.; Reniers, J.; Howey, D.A.; Tripathi, A.; Wang, Y.; Jossen, A. Ageing and efficiency aware battery dispatch for arbitrage markets using mixed integer linear programming. *Energies* **2019**, *12*, 999. [[CrossRef](#)]
14. Collath, N.; Tepe, B.; Englberger, S.; Jossen, A.; Hesse, H. Aging aware operation of lithium-ion battery energy storage systems: A review. *J. Energy Storage* **2022**, *55*, 105634. [[CrossRef](#)]
15. He, G.; Chen, Q.; Kang, C.; Pinson, P.; Xia, Q. Optimal bidding strategy of battery storage in power markets considering performance-based regulation and battery cycle life. *IEEE Trans. Smart Grid* **2015**, *7*, 2359–2367. [[CrossRef](#)]
16. Shi, Y.; Xu, B.; Tan, Y.; Kirschen, D.; Zhang, B. Optimal battery control under cycle aging mechanisms in pay for performance settings. *IEEE Trans. Autom. Control* **2018**, *64*, 2324–2339. [[CrossRef](#)]
17. Shi, Y.; Xu, B.; Wang, D.; Zhang, B. Using battery storage for peak shaving and frequency regulation: Joint optimization for superlinear gains. *IEEE Trans. Power Syst.* **2017**, *33*, 2882–2894. [[CrossRef](#)]
18. Kumtepelı, V.; Hesse, H.; Morstyn, T.; Nosratabadi, S.M.; Aunedi, M.; Howey, D.A. Depreciation Cost is a Poor Proxy for Revenue Lost to Aging in Grid Storage Optimization. *arXiv* **2024**, arXiv:2403.10617.
19. Li, Y.; Liu, K.; Foley, A.M.; Zülke, A.; Berecibar, M.; Nanini-Maury, E.; Van Mierlo, J.; Hoster, H.E. Data-driven health estimation and lifetime prediction of lithium-ion batteries: A review. *Renew. Sustain. Energy Rev.* **2019**, *113*, 109254. [[CrossRef](#)]
20. Naumann, M.; Schimpe, M.; Keil, P.; Hesse, H.C.; Jossen, A. Analysis and modeling of calendar aging of a commercial LiFePO<sub>4</sub>/graphite cell. *J. Energy Storage* **2018**, *17*, 153–169. [[CrossRef](#)]
21. Sarasketa-Zabala, E.; Gandiaga, I.; Rodriguez-Martinez, L.; Villarreal, I. Calendar ageing analysis of a LiFePO<sub>4</sub>/graphite cell with dynamic model validations: Towards realistic lifetime predictions. *J. Power Sources* **2014**, *272*, 45–57. [[CrossRef](#)]
22. Naumann, M.; Spingler, F.B.; Jossen, A. Analysis and modeling of cycle aging of a commercial LiFePO<sub>4</sub>/graphite cell. *J. Power Sources* **2020**, *451*, 227666. [[CrossRef](#)]
23. Sarasketa-Zabala, E.; Gandiaga, I.; Martinez-Laserna, E.; Rodriguez-Martinez, L.; Villarreal, I. Cycle ageing analysis of a LiFePO<sub>4</sub>/graphite cell with dynamic model validations: Towards realistic lifetime predictions. *J. Power Sources* **2015**, *275*, 573–587. [[CrossRef](#)]
24. Wicke, M.; Bocklisch, T. Hierarchical Energy Management of Hybrid Battery Storage Systems for PV Capacity Firming and Spot Market Trading Considering Degradation Costs. *IEEE Access* **2024**, *12*, 52669–52686. [[CrossRef](#)]
25. Dowling, A.W.; Kumar, R.; Zavala, V.M. A multi-scale optimization framework for electricity market participation. *Appl. Energy* **2017**, *190*, 147–164. [[CrossRef](#)]
26. Mayer, K.; Trück, S. Electricity markets around the world. *J. Commod. Mark.* **2018**, *9*, 77–100. [[CrossRef](#)]

27. 50Hertz Transmission GmbH; Amprion GmbH; TenneT TSO GmbH; TransnetBW GmbH. Basics of Balancing Services. Available online: <https://www.regelleistung.net/en-us/Basics-of-balancing-services> (accessed on 17 March 2025).
28. Dunbar, A.; Tagliaferri, F.; Viola, I.M.; Harrison, G. The impact of electricity price forecast accuracy on the optimality of storage revenue. In Proceedings of the 3rd Renewable Power Generation Conference (RPG 2014), Naples, Italy, 24–25 September 2014; IET: Stevenage, UK, 2014; pp. 1–6.
29. Van Rossum, G.; Drake, F.L., Jr. *The Python Language Reference*; Python Software Foundation: Wilmington, DE, USA, 2014.
30. Bynum, M.L.; Hackebeil, G.A.; Hart, W.E.; Laird, C.D.; Nicholson, B.L.; Sirola, J.D.; Watson, J.P.; Woodruff, D.L. *Pyomo-Optimization Modeling in Python*; Springer: Berlin/Heidelberg, Germany, 2021; Volume 67.
31. Gurobi Optimization LLC. *Gurobi Optimizer Reference Manual*; Gurobi Optimization LLC: Beaverton, OR, USA, 2023.
32. Tadayon, L.; Meiers, J.; Ibing, L.; Erdelkamp, K.; Frey, G. Coordinated operation of pumped hydro energy storage with reversible pump turbine and co-located battery energy storage system. *at-Automatisierungstechnik* **2025**, *73*, 136–144. [CrossRef]
33. 50Hertz Transmission GmbH; Amprion GmbH; TenneT TSO GmbH; TransnetBW GmbH. Präqualifikationsverfahren für Regelreserveanbieter (FCR, aFRR, mFRR) in Deutschland (“PQ-Bedingungen”). Available online: [https://www.regelleistung.net/xspproxy/api/StaticFiles/Regelleistung/Infos\\_f%C3%BCr\\_Anbieter/Wie\\_werde\\_ich\\_Regelenergieanbieter\\_Pr%C3%A4qualifikation/Pr%C3%A4qualifikationsbedingungen\\_FCR\\_aFRR\\_mFRR/PQ-Bedingungen-2024\\_07\\_05.pdf](https://www.regelleistung.net/xspproxy/api/StaticFiles/Regelleistung/Infos_f%C3%BCr_Anbieter/Wie_werde_ich_Regelenergieanbieter_Pr%C3%A4qualifikation/Pr%C3%A4qualifikationsbedingungen_FCR_aFRR_mFRR/PQ-Bedingungen-2024_07_05.pdf) (accessed on 17 March 2025).
34. 50Hertz Transmission GmbH; Amprion GmbH; TenneT TSO GmbH; TransnetBW GmbH. Datacenter. Available online: <https://www.regelleistung.net/en-us/Data> (accessed on 17 March 2025).
35. EPEX SPOT SE. Market Data. Available online: <https://www.epexspot.com/en/market-results> (accessed on 17 March 2025).
36. 50Hertz Transmission GmbH; Amprion GmbH; TenneT TSO GmbH; TransnetBW GmbH. Balancing Capacity Data. Available online: <https://www.netztransparenz.de> (accessed on 17 March 2025).
37. Schmidt, O.; Staffell, I. *Monetizing Energy Storage: A Toolkit to Assess Future Cost and Value*; Oxford University Press: Oxford, UK, 2023.
38. ISEA RWTH Aachen and Enspired GmbH. Battery Revenue Index (Beta-Version). Available online: <https://battery-charts.rwth-aachen.de/battery-revenue-index-beta-version-2/> (accessed on 17 March 2025).
39. Spotnitz, R. Simulation of capacity fade in lithium-ion batteries. *J. Power Sources* **2003**, *113*, 72–80. [CrossRef]
40. Park, J.; Appiah, W.A.; Byun, S.; Jin, D.; Ryou, M.H.; Lee, Y.M. Semi-empirical long-term cycle life model coupled with an electrolyte depletion function for large-format graphite/LiFePO<sub>4</sub> lithium-ion batteries. *J. Power Sources* **2017**, *365*, 257–265. [CrossRef]

**Disclaimer/Publisher’s Note:** The statements, opinions and data contained in all publications are solely those of the individual author(s) and contributor(s) and not of MDPI and/or the editor(s). MDPI and/or the editor(s) disclaim responsibility for any injury to people or property resulting from any ideas, methods, instructions or products referred to in the content.